Available online at www.sciencedirect.com
ScienceDirect
Journal of the European Ceramic Society 27 (2007) 3231–3238
www.elsevier.com/locate/jeurceramsoc

Crystallization behaviour, structure and properties of sintered glasses in the diopside–Ca-Tschermak system

A. Goel [a], D.U. Tulyaganov [a,b], S. Agathopoulos [a], M.J. Ribeiro [c], J.M.F. Ferreira [a,*]

[a] *Department of Ceramics and Glass Engineering, University of Aveiro, CICECO, 3810-193 Aveiro, Portugal*
[b] *Scientific Research Institute of Space Engineering, 700128 Tashkent, Uzbekistan*
[c] *UIDM, ESTG, Polytechnic Institute of Viana do Castelo, 4900 Viana do Castelo, Portugal*

Received 27 October 2006; received in revised form 12 January 2007; accepted 19 January 2007
Available online 29 March 2007

Abstract

Four glasses with nominal compositions of $CaMg_{0.8}Al_{0.4}Si_{1.8}O_6$, $CaMg_{0.75}Al_{0.5}Si_{1.75}O_6$, $CaMg_{0.7}Al_{0.6}Si_{1.7}O_6$, and $CaMg_{0.65}Al_{0.7}Si_{1.65}O_6$, were successfully obtained by melting in alumina crucibles at 1580 °C for 1 h, aiming at producing glass ceramics based on diopside–Ca-Tschermak. Sintering and crystallization behaviour of the glasses, coupled with calculation of the activation energy of crystallization, were investigated upon heat treatment under different conditions of heating rates (5–40 K/min), temperatures (850–1000 °C), and times (1–300 h). The experimental results showed that there is a threshold of Ca-Tschermak solubility in diopside structure at ca. 30 mol.%, which is technologically important with regard to the production of mono-mineral glass ceramics. The good matching of thermal properties and the strong adherence to yttria stabilized cubic zirconia indicate the investigated glass ceramics for further experimentation as candidates for SOFC sealants.

Keywords: Sintering; Microstructure final; Thermal expansion; Glass ceramics; Fuel cells

1. Introduction

The stability of clinopyroxenes over a broad spectrum of chemical compositions, in conjunction with the possibility of achieving desired physical properties and high chemical durability, have been extensively considered for producing glass ceramic (GC) materials for a large variety of applications.[1–6] Ceramics and GCs based on pyroxenes attract increasing interest in several advanced fields, such as electronics,[7,8] biomedicine,[9,10] immobilization of radioactive wastes,[11] and sealants for solid oxide fuel cells (SOFC).[12]

The chain silicate structure of pyroxenes enables solubility of various cations in their structure. The Ca–Al-bearing monoclinic pyroxene, known as Ca-Tschermak ($CaAl_2SiO_6$, hereafter briefly designated as Ts), is representative of pyroxene group, where Al is at both tetrahedral and octahedral sites.[13] The properties of GCs based on clinopyroxenes, and particularly on solid solutions of Ts and diopside ($CaMgSi_2O_6$, hereafter briefly designated as D), can be highly controlled due to their particular structural features.[1,2,8,14] The D–Ts solid solutions have a general formula of $Ca[Mg_{1-x}Al_x](Si_{1-x/2}Al_{x/2})_2O_6$, where the square brackets and the parentheses denote the octahedral and the tetrahedral sub-lattices, respectively.[13] With respect to D formula, the cation substitution in D–Ts solid solutions is governed by Tschermak's substitution, concisely represented as $(Si^{4+}) + [Mg^{2+}] \leftrightarrow (Al^{3+}) + [Al^{3+}]$. The amount of Ts in a pyroxene structure depends on the original composition of the glass and the crystallization parameters.[14–16]

In our earlier study,[12] a glass with nominal composition of $CaMg_{0.8}Al_{0.4}Si_{1.8}O_6$ (which corresponds to 80/20 D/Ts mole ratio) was derived from D with a substitution concisely represented as $0.2(Si^{4+} + Mg^{2+}) \leftrightarrow 0.4Al^{3+}$. The experimental results of differential thermal analysis (DTA) showed that the temperature of crystallization peak strongly depends on the size of glass particles, indicating that the glass is prone to surface crystallization. Bars made from glass-powder compacts (where the fine powders were obtained from milled glass frit) were almost completely sintered at 850 °C. Devitrification took place at higher temperatures (>900 °C), resulting in mono-mineral GCs of augite Au, $Ca(Mg_{0.70}Al_{0.30})(Si_{1.70}Al_{0.30})O_6$, even after

* Corresponding author. Tel.: +351 234 370242; fax: +351 234 425300.
E-mail address: jmf@cv.ua.pt (J.M.F. Ferreira).

0955-2219/$ – see front matter © 2007 Elsevier Ltd. All rights reserved.
doi:10.1016/j.jeurceramsoc.2007.01.018

Table 1
Compositions of the parent glasses

	MgO	CaO	SiO_2	Al_2O_3
DT1, $CaMg_{0.8}Al_{0.4}Si_{1.8}O_6$ (D/Ts = 80/20)				
wt.%	14.87	25.86	49.87	9.40
mol.%	21.05	26.32	47.37	5.26
Mole ratio	4	5	9	1
DT1a, $CaMg_{0.75}Al_{0.5}Si_{1.75}O_6$ (D/Ts = 75/25)				
wt.%	13.93	25.85	48.47	11.75
mol.%	19.99	26.67	46.67	6.67
Mole ratio	3	4	7	1
DT1b, $CaMg_{0.7}Al_{0.6}Si_{1.7}O_6$ (D/Ts = 70/30)				
wt.%	13.00	25.84	47.06	14.09
mol.%	18.92	27.03	45.95	8.11
Mole ratio	2.33	3.33	5.67	1
DT1c, $CaMg_{0.65}Al_{0.7}Si_{1.65}O_6$ (D/Ts = 65/35)				
wt.%	12.07	25.83	45.66	16.44
mol.%	17.81	27.40	45.20	9.59
Mole ratio	1.86	2.86	4.71	1

One weight percent NiO was added to the batches.

prolonged heat treatment (50 h at 900 °C). Mono-mineral GCs have predictable advantages for applications involving thermal cycling, like as sealing materials for SOFC. As a matter of fact, the sealing in planar SOFC design is often carried out using GCs as they are typically chemically and mechanically stronger than glass seals. Feasibility of single phase solid solutions is very important to satisfy severe requirements for SOFC sealing materials operating at 600–1000 °C for thousands of hours under both oxidising and reducing atmospheres.

The present work extrapolated that glass composition towards three new glasses with compositions corresponding to different D/Ts mole ratios. To be consistent with the previous study,[12] where the composition with D/Ts ratio of 80/20 was designated as DT1, the three new compositions are designated as DT1a for D/Ts = 75/25 ($CaMg_{0.75}Al_{0.5}Si_{1.75}O_6$), DT1b for D/Ts = 70/30 ($CaMg_{0.7}Al_{0.6}Si_{1.7}O_6$), and DT1c for D/Ts = 65/35 ($CaMg_{0.65}Al_{0.7}Si_{1.65}O_6$). Table 1 presents detailed information of all these compositions. (In the present study, the DT1 was also prepared and characterized in the same course with the other three glasses.) The incorporation in the batches of NiO (1 wt.%) was considered to improve the adhesion of the resultant GCs to the metallic components of SOFC.

The experimental results and their discussion address themselves to the crystallization behaviour of the glasses, the properties, the crystalline structure, and the microstructure of the sintered GCs produced after non-isothermal (at different temperatures between 850 °C and 1000 °C for 1 h) and isothermal (at 900 °C for different times up to 300 h) heat treatments, as well as a first evaluation of the potential of the new compositions as candidate for SOFC-sealant materials, with regard to the matching and adherence to yttria stabilized cubic zirconia (8YSZ).

2. Materials and experimental procedure

Powders of technical grade SiO_2 (purity >99.5%) and $CaCO_3$ (>99.5%), and of reactive grade Al_2O_3, $MgCO_3$, and NiO were used. Homogeneous mixtures of batches (∼100 g), obtained by ball milling, were preheated at 900 °C for 1 h for decarbonization and then melted in alumina crucibles at 1580 °C for 1 h, in air.

Glasses in bulk form were produced by pouring the melts on preheated bronze moulds following by annealing at 550 °C for 1 h. The samples of the glass-powder compacts were produced from glass frit, which was obtained by quenching of the glass melts in cold water. The frit was dried and then milled in a high-speed agate mill. The obtained powders had specific surface area 1.26–1.37 m^2/g (measured by BET technique, Micromeritics, Gemini II 2370, USA). The fine glass powder was granulated (by stirring in a mortar) in a 5 vol.% polyvinyl alcohol solution (PVA, Merck; the solution of PVA was made by dissolution in warm water) in a proportion of 97.5 wt.% of glass powder and 2.5 wt.% of PVA solution. Rectangular bars with dimensions of 4 mm × 5 mm × 50 mm were prepared by uniaxial pressing (80 MPa). The bars were sintered under non-isothermal conditions for 1 h at 850 °C, 900 °C, 950 °C, and 1000 °C, and under isothermal conditions at 900 °C for 50 h, 100 h, and 300 h. A slow heating rate of 2 K/min aimed to prevent deformation of the samples.

To investigate the adherence of the new compositions to cubic zirconia (applied as electrolyte in SOFC), wetting experiments between glass powders and fine polished flat pellets of cubic zirconia (8% yttria fully stabilized, TOSOH, Japan) were carried out at 900 °C for 100 h in air. Moreover, samples obtained by uniaxial pressing (80 MPa) of 8YSZ powder and the glass powders (1:1, w/w) were heat treated under similar conditions.

Besides BET, the following techniques were also employed. Dilatometry measurements were done with prismatic samples with cross-section of 4 mm × 5 mm (Bahr Thermo Analyse DIL 801 L, Germany; heating rate 5 K/min). Differential thermal analysis of the fine powders was carried out in air (DTA-TG, Labsys Setaram, France). To calculate the activation energy of crystallization, fine glass powders of 50 mg were heated up to 1000 °C with different heating rates (β) of 5 K/min,

20 K/min, 30 K/min, and 40 K/min. The crystalline phases were determined by X-ray diffraction (XRD) analysis (Rigaku Geigerflex D/Mac, C Series, Cu Kα radiation, Japan). Copper Kα radiation (λ = 1.5406 nm), produced at 30 kV and 25 mA, scanned the range of diffraction angles (2θ) between 10° and 80° with a 2θ-step of 0.02°/s. The phases were identified by comparing the obtained diffractograms with patterns of standards complied by the International Centre for Diffraction Data (ICDD). Microstructure observations were done at polished (mirror finishing) and then etched (by immersion in 2 vol.% HF solution during 20,120 s) surfaces of samples (in the case of zirconia/glass interfaces, cross-sections were first done) by field emission scanning electron microscopy (FE-SEM, Hitachi S-4100, Japan; 25 kV acceleration voltage, beam current 10 μA) under secondary electron mode. Archimedes' method (i.e. immersion in diethyl phthalate) was employed to measure the apparent density of the samples. The mechanical properties were evaluated by measurements of three-point bending strength of rectified parallelepiped bars (3 mm × 4 mm × 50 mm) of sintered GCs (Shimadzu Autograph AG 25 TA; 0.5 mm/min displacement). The linear shrinkage during sintering was calculated from the difference of the dimensions between the green and the sintered bars. The mean values and the standard deviations presented for shrinkage, density, and bending strength have been obtained from (at least) 10 different samples.

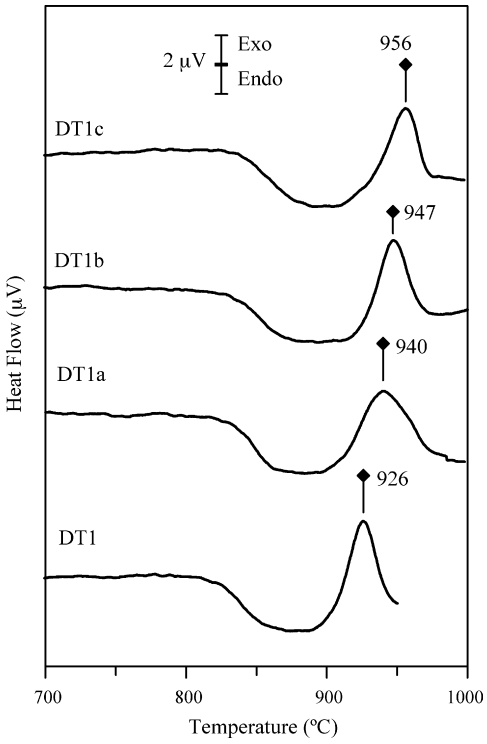

Fig. 1. Differential thermal analysis (DTA) of fine powders of the investigated glasses heated with a rate of 5 K/min.

3. Results and discussion

3.1. Characterization of glasses

3.1.1. Thermal analysis

Melting at 1580 °C for 1 h was adequate to obtain highly homogenous molten glasses for all the investigated compositions, which, after casting, resulted in bubble-free, homogenous, transparent glasses with a dark colour of honey (likely due to NiO). Absence of crystalline inclusions was also confirmed by X-ray and SEM analyses, afterwards.

The glass transition (T_g) and softening points (T_s) were determined together with the linear thermal expansion coefficients (CTE) from the slope of the linear part of the dilatation curves (200–500 °C) (not shown). The results, presented in Table 2, indicate that both T_g and T_s range within narrow temperature intervals (660–670 °C and 700–720 °C, respectively), but there is no evidence of systematic influence of D/Ts mole ratio on these values.

Table 2
Characteristic temperatures and thermal expansion coefficients (CTE) of the investigated glasses, determined by thermal analyses with a heating rate of 5 K/min

	DT1	DT1a	DT1b	DT1c
T_g (°C)	667	668	660	670
T_s (°C)	710	715	700	720
T_p (°C)	926	940	947	956
CTE ($\times 10^{-6}$ K^{-1}) (200–500 °C)	7.22	7.89	7.31	7.66

The plots of DTA in Fig. 1, obtained from fine powders with heating rate of 5 K/min, feature a single strong exothermic peak, attributed to crystallization. The temperatures of the peak (T_p), listed in Table 2, depend on D/Ts mole ratio since they increase from glass DT1 to glass DT1c. It should be noted that there is a difference of the T_p values for the glass DT1 recorded in this study and in the earlier one,[12] attributed to the use of different DTA equipment.

3.1.2. Activation energy of crystallization

To calculate the activation energy of crystallization, the experimental results of DTA with different heating rates (β = 5 K/min, 20 K/min, 30 K/min, and 40 K/min) were applied in the modified forms of Kissinger (Eq. (1)) and Ozawa (Eq. (2)) equations:

$$\ln\left(\frac{T_p^2}{\beta^n}\right) = \frac{E_a}{RT_p} + \text{constant} \quad (1)$$

$$\ln\beta = -\frac{mE_a}{nRT_p} + \text{constant} \quad (2)$$

where n is the Avrami constant, and m is the crystal growth dimensionality. These equations, established by Matusita and Sakka,[17] assume that nucleation does not occur during crystal growth, and crystal growth is interface controlled. Our earlier study[12] has experimentally demonstrated that these glasses are prone to surface crystallization. Hence, the high surface nucleation rate can allow the assumption that all surface nuclei form before crystal growth and no new nuclei form during grow-

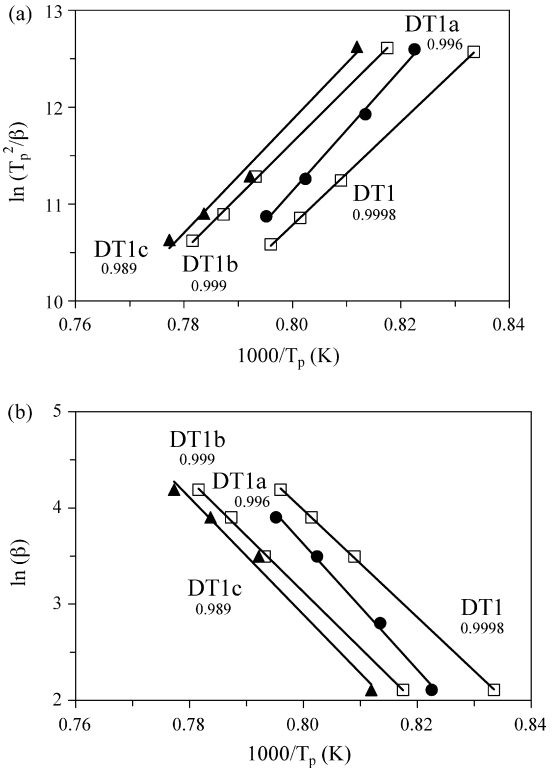

Fig. 2. Plots according to the modified (a) Kissinger (Eq. (1)) and (b) Ozawa (Eq. (2)) equations for determination of the activation energy for crystallization of the investigated glasses (E_a). The values or correlation coefficients (r^2) are also presented.

ing. In that case, the values of n and m in Eqs. (1) and (2) can be considered both equal to 1 that is the case for surface crystallization.[17]

Accordingly, the linear fitting (with the least square method) of the experimental results to Eqs. (1) and (2) for the four investigated glasses is shown (together with the correlation coefficients, r^2) in Fig. 2a and b, respectively. The values of E_a, calculated from these plots, are presented in Table 3. The high values of correlation coefficients support the validity of Kissinger method[18] as well as the validity of our above assumptions. The two methods (Kissinger and Ozawa) yielded quite similar E_a values for each composition, which usually happens in cases of weak dependence of T_p on heating rate.[19] The values of Table 3 agree to E_a values reported for glasses with composition of diopside (573 kJ/mol)[20] and diopside–anorthite (367–670 kJ/mol),[21] which are also prone to surface crystallization.

Table 3
Activation energy for crystallization of the investigated glasses calculated by Eqs. (1) and (2) and the plots of Fig. 3 (kJ/mol)

Glass	E_a (Kissinger)	E_a (Ozawa)
DT1	442.56	440.24
DT1a	522.57	516.48
DT1b	464.04	461.02
DT1c	485.46	481.51

3.2. Evolution of crystalline phases

3.2.1. Non-isothermal conditions 850–1000 °C (1 h)

The evolution of crystalline regime of the glass-powder compacts over increasing temperature (always for 1 h) is demonstrated in the X-ray diffractograms of Fig. 3, while characteristic microstructures (observed by SEM) are shown in Fig. 4 (the diffractograms of DT1 are not shown, because there were no significant differences with our earlier study).[12] There were evidences of crystallization in the bars of DT1a, DT1b, and DT1c compositions (Fig. 3) sintered at 850 °C, whereas DT1 samples remained amorphous at the same temperature.[12] Augite (designated as Au, ICDD card 01-078-1392, $CaMg_{0.70}Al_{0.30}Si_{1.70}Al_{0.30}O_6$) was identified in DT1a and DT1b. Devitrification was seemingly more intensive in the case of DT1a, enough to have an impact in the microstructure where first crystals embedded in the glassy matrix can be observed (Fig. 4a). In the composition DT1c calcium plagioclase anorthite (designated as An, ICDD card 00-041-1486, $CaAl_2Si_2O_8$) was also registered. Heat treating at higher temperatures 900–1000 °C significantly improved the crystallinity in all investigated compositions concluded from the increasing intensity of the XRD peaks (Fig. 3). Mono-mineral GCs composed exclusively of augite were obtained for the case of DT1,[12] DT1a, and DT1b evidencing solubility of Ts molecule in the structure

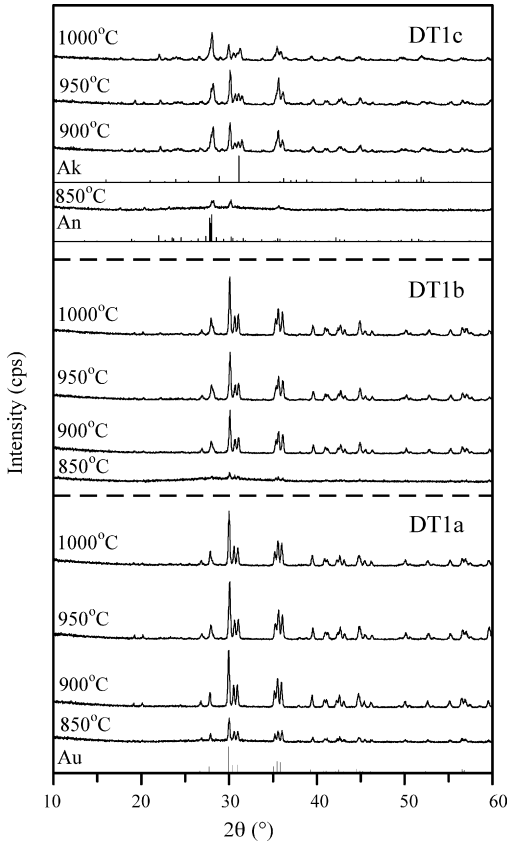

Fig. 3. X-ray diffractograms of glass-powder compacts of DT1a, DT1b, and DT1c, after heat treatment at different temperatures for 1 h. (Au: augite ICDD card 01-078-1392; An: anorthite 00-041-1486; Ak: akermanite 00-035-592. The spectra have not been normalized. Full scale of intensity axes 13,000 cps.)

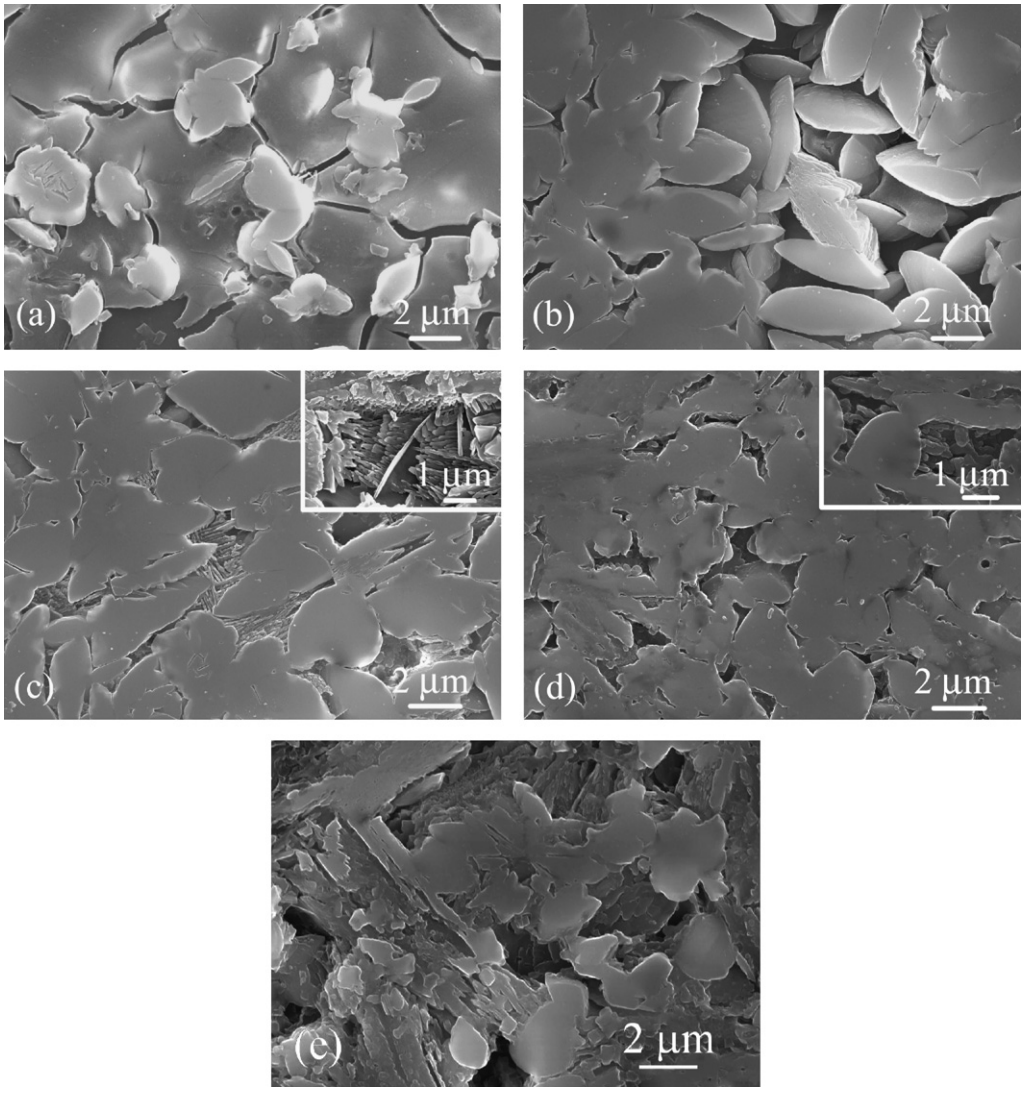

Fig. 4. Microstructure (revealed after chemical etching of polished surfaces with HF solution) of the glass ceramics DT1a heat treated at (a) 850 °C, (b) 900 °C, and (c) 950 °C; DT1b at 950 °C (d) and DT1c at 900 °C (e).

of D and formation of D–Ts solid solutions. Microstructure of GCs DT1a, and DT1b (Fig. 4b–d) resembles the microstructure of GC DT1[12] where the oval shaped crystals of augite phase (2–3 μm in length) are closely bordering each other. From the inserted images in Fig. 4c and d the finer augite crystals (less than 1 μm in length) can be observed in the inner part of the glass ceramics.

Augite is the most widespread member of pyroxenes and represents a group of closely related minerals with chemical formula of $Ca(Mg,Fe,Al)(SiAl)O_6$, identical in structure, but containing different percentages of certain elements.[1,3] In the light of the experimental results of the present study, augite (that was obviously Fe-free) seemingly acts as an intermediary member between D and Ts, representing a mineral midway between these two minerals along this series, where Al^{3+} occupies both octahedral (AlO_6) and tetrahedral (AlO_4) positions in the structure.

The above mentioned ICDD card 01-078-1392, which had the most precise fitting to the diffractograms of Fig. 3, corresponds to augite crystallized in monoclinic structure with lattice parameters $a = 9.717$ nm, $b = 8.882$ nm, $c = 5.266$ nm, and $\beta = 106.16°$.[22] However, there is also another ICDD card of augite (01-078-1391)[23] whose formula, $Ca(Mg_{0.85}Al_{0.15})(Si_{1.70}Al_{0.30})O_6$, corresponds to 22.5 mol.% Ts dissolved in D, which matches fairly well to the D/Ts solid solutions of the parent glasses of the present study. Since the differences between the patterns of the two ICDD cards are very small, therefore, only one ICDD card 01-078-1392 has been used in XRD diffractograms. However, to investigate the distribution of aluminium in the tetrahedral and octahedral sub-lattices of D/Ts solid solutions, other experimental techniques (e.g. Mossbauer, MAS NMR, etc.), or statistical–thermodynamic models need to be applied.

The above experimental results (obtained by studying glass crystallization between 850 °C and 1000 °C for 1 h) suggest a solubility limit of Ts in D at about 30 mol.% Ts. This limit was justified by the behaviour of the glass DT1c (i.e. D/Ts = 65/35) at which except augite phase anorthite and akermanite (designated

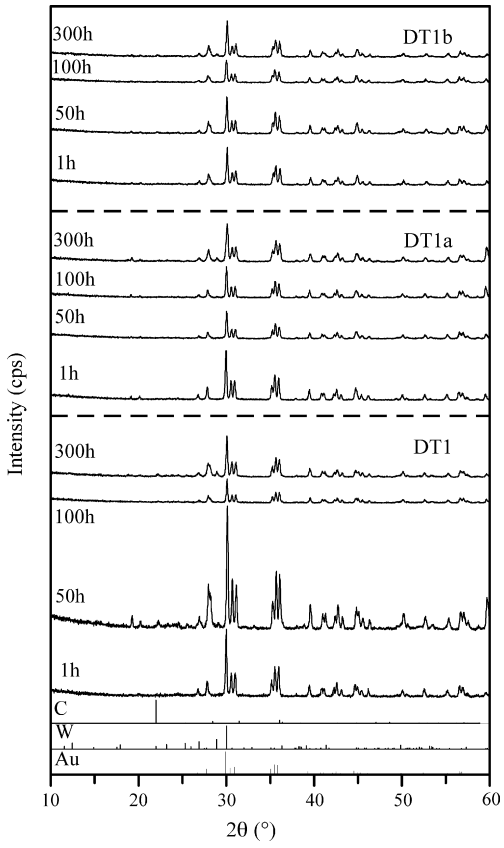

Fig. 5. X-ray diffractograms of glass-powder compacts of DT1, DT1a, and DT1b, after heat treatment at 900 °C for 1 h, 50 h, 100 h, and 300 h. (Au: augite ICDD card 01-078-1392; W: wollastonite 00-042-0550; C: cristobalite 00-039-1425. The spectra have not been normalized. Full scale of intensity axes 15,000 cps.)

as Ak, ICDD card 00-035-592 $Ca_2MgSi_2O_7$) where precipitated at temperatures 850 °C and 900 °C, respectively. The SEM image of GC DT1c (Fig. 4e) is noticeably different from those of GCs DT1, DT1a, and DT1b: apart from augite, prismatic blade shaped crystals, a typical characteristic of anorthite phase are presented. It is worthy noting that the range of D/Ts solid solutions is more spread in the natural Si-poor pyroxene rocks that can contain even 50 mol.% Ts.[13] Continuous D–Ts solid solutions have been obtained when glass crystallization was achieved by applying pressure of 2 GPa at 1400 °C for 24 h.[13]

3.2.2. Isothermal conditions (900 °C)

The stability of crystalline regime of the mono-mineral GCs DT1, DT1a, and DT1b, under prolong isothermal heat treatment at 900 °C (that is about −100 °C higher than the operation temperature of SOFC) for 50 h, 100 h, and 300 h, is demonstrated in X-ray diffractograms of Fig. 5. Comparison of the intensity of the peaks suggest that exposure of the samples beyond 50 h at 900 °C causes a decay of their crystallinity, which is striking in DT1, less pronounce in DT1b, and negligible in DT1a. Augite, which probably dissolves in the glassy phase, seemingly recrystallizes after 300 h, since the intensity of peaks increase. Careful observation of diffractograms may suggest evidence of partial destabilization of augite since low intensity peaks of cristobalite (designated as C, ICDD card 00-039-1425, SiO_2) after 100 h for DT1 and DT1b, and wollastonite (designated as W, ICDD card 00-042-0550 $CaSiO_3$) after 300 h for all compositions were developed.

3.3. Properties of sintered glass ceramics

3.3.1. Shrinkage, density, and bending strength

Sintering generally starts at temperatures slightly higher than T_g and occurs due to viscous flow, which instigates coalescence of powder and removes the pores from the bulk of materials. In the case of the four investigated compositions (Table 1), the glass-powder compacts resulted in mostly amorphous (Fig. 3) but highly dense sintered samples of dark brown colour after heat treatment at 850 °C. Sintering preceded crystallization (Figs. 1 and 3) suggesting that densification was complete at 900 °C, where the investigated samples exhibited white colour. The values of shrinkage, density, and bending strength of glass-powder compacts sintered at different temperatures for 1 h, summarized in Table 4, support fairly well the above suggested

Table 4
Values of properties of the glass ceramics produced from glass-powder compacts after heat treatment at different temperatures for 1 h

Composition	850 °C	900 °C	950 °C	1000 °C
Shrinkage (%)				
DT1	15.20 ± 0.31	15.88 ± 0.39	15.90 ± 0.90	15.74 ± 0.16
DT1a	15.92 ± 0.27	16.37 ± 0.13	16.12 ± 0.45	16.18 ± 0.05
DT1b	15.86 ± 0.22	16.29 ± 0.06	16.18 ± 0.38	15.67 ± 0.08
DT1c	15.22 ± 0.57	16.20 ± 0.37	15.61 ± 0.19	16.03 ± 0.08
Density (g/cm^3)				
DT1	2.80 ± 0.01	2.96 ± 0.01	2.95 ± 0.01	2.94 ± 0.01
DT1a	2.91 ± 0.01	2.94 ± 0.01	2.94 ± 0.01	2.94 ± 0.01
DT1b	2.86 ± 0.01	2.94 ± 0.01	2.93 ± 0.01	2.93 ± 0.01
DT1c	2.85 ± 0.01	2.86 ± 0.01	2.86 ± 0.01	2.86 ± 0.01
Bending strength (MPa)				
DT1	90.56 ± 16.77	189.06 ± 10.28	165.30 ± 17.13	165.18 ± 2.90
DT1a	77.34 ± 7.84	170.01 ± 18.49	154.65 ± 17.53	158.24 ± 12.20
DT1b	91.77 ± 26.77	137.97 ± 19.45	126.69 ± 14.16	155.45 ± 7.64
DT1c	105.13 ± 20.97	69.92 ± 6.37	51.78 ± 5.24	13.40 ± 8.40

stages, occurring over increasing temperature. Further increase of temperature up to 950 °C or 1000 °C had negligible influence on density, but shrinkage showed a tendency to decrease.

A general trend of decreasing the values of density and bending strength with increasing the amount of Ts can be suggested. The high crystallinity of GC DT1 (Fig. 5) that correlates with its respectively low E_a value should be responsible for the best mechanical performance along the heat treatment at 900–1000 °C for 1 h. Furthermore, the results of Table 4 underline the importance of producing mono-mineral GCs. The properties of DT1c GCs were significantly poorer than all the other mono-mineral investigated GCs. The simultaneous presence of three crystalline phases in DT1c GCs (anorthite, augite, akermanite, Fig. 3) anticipates a detrimental impact (with regard to the structural integrity of GC) of the mismatch of CTE of each phase during cooling.

3.3.2. Adherence to zirconia (8YSZ)

The good matching of the CTEs values (200–700 °C) between the GCs and zirconia, calculated form the slope of these lines (not shown) and presented in Table 5, qualify the GCs DT1, DT1a and DT1b for further experimentation as candidate SOFC-sealant materials. However, as has been observed with other GCs applied for sealing SOFC,[24,25] prolong isothermal heat treatment at 900 °C for 300 h caused a decrease of CTE values, as shown in Table 5 (except DT1c). In the present study, this reduction can be attributed to the above suggested dissolution–recrystallization processes (Fig. 5).

A characteristic microstructure of the interface formed between 8YSZ pellet and glass-powder DT1b after heat treatment at 900 °C for 100 h in air is shown in Fig. 6. Similar interfaces were observed with the glasses DT1 and DT1a. The good matching of the CTEs of zirconia and DT1b resulted in a generally continuous interface with no cracks or gaps, despite the extensive crystallization of DT1b (see the similarities of microstructure of DT1b in Figs. 4d and 6). There is no evidence of formation of a reaction zone at the interface, which, if existed, should be quite wide due to the long heat treatment. The absence of reaction product between the glasses and zirconia was also confirmed by X-ray analysis of samples made of powder mixtures of glasses and 8YSZ similarly heat treated (i.e. 900 °C, 100 h), where only augite and 8YSZ (ICDD card 01-082-1245) were identified. The above features, in conjunction with the fact of the prolong heat treatment, do not allow the presentation of a certain contact (wetting) angle value, but the *in situ* observed wetting angle generally indicated a good wetting regime (i.e. $\theta < 90°$).

Table 5
Thermal expansion coefficients (CTE, $\times 10^{-6}\,K^{-1}$) of the glass ceramics produced at different conditions together with the CTE of yttria stabilized cubic zirconia (8YSZ)

Composition	950 °C, 1 h	900 °C, 300 h
DT1	9.57	8.16
DT1a	8.67	8.21
DT1b	9.78	8.41
DT1c	7.28	8.01
8YSZ	10.01	

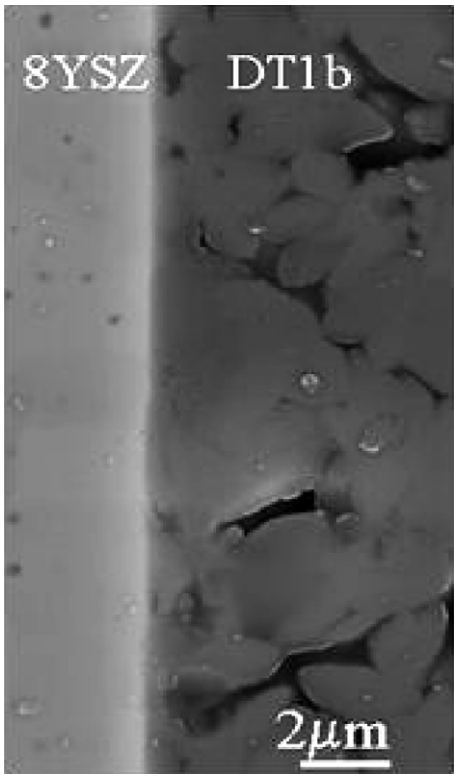

Fig. 6. Microstructure of interface between solid zirconia (8YSZ) pellet and glass DT1b, developed after heat treatment at 900 °C for 100 h.

4. Conclusions

Four glasses with nominal compositions corresponding to diopside/Ca-Tschermak mole ratios of 80/20 (DT1), 75/25 (DT1a), 70/30 (DT1b), and 65/35 (DT1b) were investigated. The experimental results showed that the D/Ts mole ratio did not systematically influence T_g and T_s, but T_p, which increased with the increase of Ca-Tschermak content. Densification is complete at 900 °C and precedes crystallization. The calculation of activation energy of crystallization supports experimental results of earlier studies whereby the investigated glasses are prone to surface crystallization. The threshold of Ca-Tschermak dissolution in diopside is ca. 30 mol.% between 850 °C and 1000 °C. This is important for obtaining mono-mineral glass ceramics of augite and their properties, such as densification, mechanical, and thermal properties.

The above experimental results in conjunction with the good matching of CTEs and the adherence of the investigated compositions with cubic zirconia (8YSZ) reveal promising perspectives for their potential as SOFC sealants. Destabilization of augite and CTE decrease after prolong heat treatment seem to be two drawbacks needed for thorough consideration in future investigations, but in the light of the general trend for decreasing SOFC operation temperatures (that are presently between 750 °C and 800 °C), the investigated compositions indicate promising prospects as candidate SOFC sealants.

Acknowledgements

The financial support of CICECO (A. Goel) and FCT (S. Agathopoulos, project SFRH/BPD/1619/2000) are gratefully acknowledged.

References

1. Pavlushkin, N. M., *Principals of Glass Ceramics Technology* (*2nd ed.*). Stroiizdat, Moscow, 1979 [in Russian].
2. Strnad, Z., *Glass-Ceramic Materials*. Elsevier, Amsterdam, 1986.
3. Zhunina, L. A., Kuzmenkov, M. I. and Yaglov, V. N., *Pyroxene Glass-Ceramics*. University of Minsk, 1974 [in Russian].
4. Barbieri, L., Bonamartini, A. C. and Lancellotti, A. C., Alkaline and alkaline earth silicate glasses and glass-ceramics from municipal and industrial wastes. *J. Eur. Ceram. Soc.*, 2000, **20**, 2477–2483.
5. Karamanov, A., Pelino, M. and Hreglich, A., Sintered glass-ceramics from municipal solid waste incinerator fly ashes. Part I. The influence of the heating rate on the sinter crystallization. *J. Eur. Ceram. Soc.*, 2003, **23**, 817–832.
6. Torres, F. J. and Alarcon, J., Mechanism of crystallization of pyroxene-based glass-ceramic glazes. *J. Non-Cryst. Solids*, 2004, **34**, 45–51.
7. Partridge, G., Elyard, M. and Budd, M. I., Glass-ceramics in substrate applications. In *Glasses and Glass-Ceramics*, ed. M. H. Levis. Chapman and Hall, London, UK, 1989, pp. 226–271.
8. Höland, W. and Beall, G. N., *Glass-Ceramic Technology*. The Am. Ceram. Soc, Westerville, OH, 2002.
9. Kobayashi, T., Okada, K., Kuroda, T. and Sato, K., Osteogenic cell cytoxicity and biomechanical strength of the new ceramic diopside. *J. Biomed. Mater. Res.*, 1997, **37**, 100–107.
10. Nonami, T. and Tsutsumi, S., Study of diopside ceramics for biomaterials. *J. Mater. Sci.: Mater. Med.*, 1999, **10**, 475–479.
11. Donald, I. W., Metcalfe, B. L. and Taylor, R. N. J., The immobilization of high level radioactive wastes using ceramics and glasses. *J. Mater. Sci.*, 1997, **32**, 5851–5887.
12. Goel, A., Tulyaganov, D. U., Agathopoulos, S., Ribeiro, M. J. and Ferreira, J. M. F., Diopside–Ca-Tschermak clinopyroxene based glass-ceramics processed via sintering and crystallization of glass powder compacts. *J. Eur. Ceram. Soc.*, 2007, **27**, 2325–2331.
13. Flemming, R. L. and Luth, R. W., ^{29}Si MAS NMR study of diopside–Ca-Tschermak clinopyroxenes: detecting both tetrahedral and octahedral Al substitution. *Am. Miner.*, 2002, **87**, 25–36.
14. Salama, S. N., Darwish, H. and Abo-Mosallam, H. A., Crystallization and properties of glasses based on diopside–Ca-Tschermak's–fluorapatite system. *J. Eur. Ceram. Soc.*, 2005, **25**, 1133–1142.
15. Kushiro, Y., Clinopyroxenes solid solutions. Part 1. The $CaAl_2SiO_6$ component. *Jpn. J. Geol. Geogr.*, 1962, **33**, 2–4.
16. Schairer, J. F. and Yoder Jr., H. S., Crystal and liquid trends in simplified alkali basalts. *Year Book*, 1964, **63**, 64–74.
17. Matusita, K. and Sakka, S., Kinetic study on crystallization of glass by differential thermal analysis—Criterion on application of Kissinger plot. *J. Non-Cryst. Solids*, 1980, **38/39**, 741–746.
18. Kissinger, H. E., Reaction kinetics in differential thermal analysis. *Anal. Chem.*, 1957, **29**, 1702–1706.
19. Hayward, P. J., Vance, E. R. and Doern, D. C., DTA/SEM study of crystallization in sphene glass-ceramics. *Am. Ceram. Soc. Bull.*, 1987, **66**, 1620–1626.
20. Branda, F., Costantini, A. and Buri, A., Non-isothermal devitrification behaviour of diopside glass. *Thermochim. Acta*, 1993, **217**, 207–212.
21. Barbieri, L., Bondioli, F., Lancellotti, I., Leonelli, C. and Montorsi, M., The anorthite-diopside system: structural and divitrification study. Part II. Crystallinity analysis by the Rietveld-RIR method. *J. Am. Ceram. Soc.*, 2005, **88**, 3131–3136.
22. ICDD card of augite 01-078-1392.
23. ICDD card of augite 01-078-1391.
24. Weil, K. S., The state-of-the-art in sealing technology for SOFC. *JOM*, 2006, 37–44.
25. Brochu, M., Gauntt, B. D., Shah, R. and Loehman, R. E., Comparison between micrometer- and nano-scale glass composites for sealing SOFC. *J. Am. Ceram. Soc.*, 2006, **89**, 810–816.